Eur. Phys. J. B **48**, 47–53 (2005)
DOI: 10.1140/epjb/e2005-00379-8

THE EUROPEAN PHYSICAL JOURNAL B

Stress in polycrystalline GaN films prepared by r.f sputtering

M. Pal Chowdhury, R.K. Roy, S.R. Bhattacharyya, and A.K. Pal[a]

Department of Materials Science, Indian Association for the Cultivation of Science, Calcutta-700 032, India

Received 25 June 2005
Published online 9 December 2005 –

Abstract. Undoped, Be-doped and Si-doped polycrystalline GaN films were deposited by R.F. sputtering onto fused silica substrates. The films were deposited at various deposition temperatures ranging from 300 K to 623 K and characterized by optical measurements while the microstructural information was obtained from SEM and XRD studies. The compositional study for the GaN film was carried out using SIMS. Residual stresses in these films were evaluated from the band tail of the absorption spectra as well as from direct measurements of hardness by commercially available depth sensing indentometer. It was observed that undoped GaN films had the highest hardness followed by that for Be-doped and Si-doped films. The values of hardness obtained form the above optical measurement tallied quite well with those obtained from direct indentation measurement.

PACS. 81.05.Ea III-V semiconductors – 78.20.-e Optical properties of bulk materials and thin films – 62.20.-x Mechanical properties of solids

1 Introduction

The use of polycrystalline semiconductors in general had attracted much interest in an expanding variety of applications in electronic and opto-electronic devices [1–3]. The main technological interest in the polycrystalline based devices lie in its very low-cost production and possibility of using low-cost substrates. Survey of literature indicates that not very many studies are reported so far on GaN in polycrystalline form. Only in recent years, some groups explored the feasibility of obtaining polycrystalline GaN layers [4-6]. The devices based on GaN epilayers suffered a setback due to the presence of biaxial strain component originating from the growth on lattice mismatched substrates with different thermal expansion coefficients and hydrostatic strains originating from incorporation of point defects altering the material's lattice constant [7,8]. Polycrystalline semiconductor films are known to contain residual stress of the order of 10^9–10^{11} $\mathrm{N\,m^{-2}}$. The nature of the stress (tensile or compressive) depends on the deposition temperature and the sign of the misfit factor between the substrate and the film [9–12]. The stress field results in higher concentration of dislocations or defects at the grain boundary. The presence of these disorder or defect states would cause a random spatial potential fluctuation (together with band gap fluctuation) which in turn would provide an excess optical absorption in the below band gap region. Therefore, if the amount of defect states present in the grain boundary region of a ploycrystalline film could be obtained from the below-band-gap optical absorption traces, one may estimate the corresponding stress or strain and hence the microhardness of the film [13–16].

In this communication, we present the synthesis of polycrystalline GaN films (doped and undoped) deposited onto fused silica (quartz) substrates kept at different temperatures by r.f. sputtering technique and evaluate the stress present in these films from the modification of the band edge absorption due to the presence of inherent electric field and mechanical stress in the grain boundary regions.

2 Experimental details

Polycrystalline GaN in thin film form was deposited onto fused silica substrates by r.f. sputtering of a GaN target (99.999%) target in argon plasma at a system pressure of ∼0.5 Pa. p- and n-doped GaN films were also deposited by using targets containing 1 at % Be and 1 at % Si in GaN respectively. The films were deposited at four different substrate temperature ($T_s \sim 300$, 423, 523 and 623 K) and for a fixed deposition time of ∼2 h. The substrates were placed on a heavy circular copper block that could be heated by appropriate heating coils passed through holes laterally drilled through the copper block. The temperature of the substrates could be monitored and controlled by a copper-constant thermocouple by an on/off electronic temperature controller. Before starting the actual deposition, the target was pre-sputtered with a shutter located in

[a] e-mail: msakp@iacs.res.in

between the target and the substrate. All the depositions were performed with a 140 W R.F. power from a power supply capable of delivering 1.0 KW, 13.56 MHz. The distance between the target (2.5 cm dia) and substrate was ∼3.5 cm. Optical studies were performed by measuring transmittance at room temperature in the wavelength region $\lambda = 200$–800 nm using a spectrophotometer (Hitachi-U3410). The spectra were recorded with a resolution of $\lambda \sim 0.07$ nm along with a photometric accuracy of ±0.3% for transmittance measurements. SEM images were obtained with a JEOL scanning transmission electron microscope. Depth sensitive indentation (DSI) technique has recently emerged as a powerful tool to characterize the near-surface mechanical properties of materials, particularly thin films, super hard protective films and coatings including ceramic thermal barrier coatings [17–19]. The hardness measurements were carried out by using the depth sensing indentometer, fully automated FISCHERSCOPE H100CXY$_p$ with a XY programmable stage utilizing a low load range between 1 and 30 mN such as to ensure that the maximum depth of penetration of the indenter does not exceed 10% of the film thickness. The hardness values measured by this machine are in full compliance with standards like DIN 50359 and DIN EN ISO 14577. The test force range available in the machine was 0.4–1000 mN with a resolution of 0.2 μN. Similarly, the measurement of penetration depth carried out by the machine with a resolution of 0.1 nm.

3 Results and discussion

3.1 Optical properties

The absorption coefficients (α) of the doped and undoped GaN films were determined by measuring transmittance and reflectance in these films [19–22]. In general, the absorption coefficient (α) may be written as a function of the incident photon energy ($h\nu$) so that:

$$\alpha = (A/h\nu)\{h\nu - E_g\}^m \tag{1}$$

where A is a constant which is different for different transitions indicated by different values of m and E_g is the corresponding band gap.

Now,

$$\ln(\alpha h\nu) = \ln A + m\ln(h\nu - E_g) \tag{2}$$

and

$$\frac{d\left[\ln\left(\alpha h\nu\right)\right]}{d\left[h\nu\right]} = \frac{m}{h\nu - E_g}. \tag{3}$$

Equation (3) suggests that a plot of d[ln($\alpha h\nu$)]/d[$h\nu$] versus $h\nu$ will indicate a divergence at $h\nu = E_g$ from which the value of E_g may be obtained. Once E_g is found, the value of m can easily be calculated (Eq. (2)) from the slope of the plot of ln($\alpha h\nu$) versus ln($h\nu - E_g$). Figure 1 (inset) shows the plot of ln($\alpha h\nu$) versus ln($h\nu - E_g$) for a representative film (undoped GaN film) from which one can obtain the value of $m \sim 0.51$ indicating direct transition. The band gap was determined by extrapolating the linear portion of the plot of $(\alpha h\nu)^2$ versus $h\nu$ (Fig. 1) and are shown in Table 1 for all the films studied here. It may be noted here that the films deposited at higher substrate temperature during deposition had lower band gaps. It was also observed that films deposited at >600 K had predominant cubic phase while the films deposited at temperatures below 350 K were found to be hexagonal. Films deposited at intermediate temperature contained both the hexagonal and cubic phases. Band gap for both

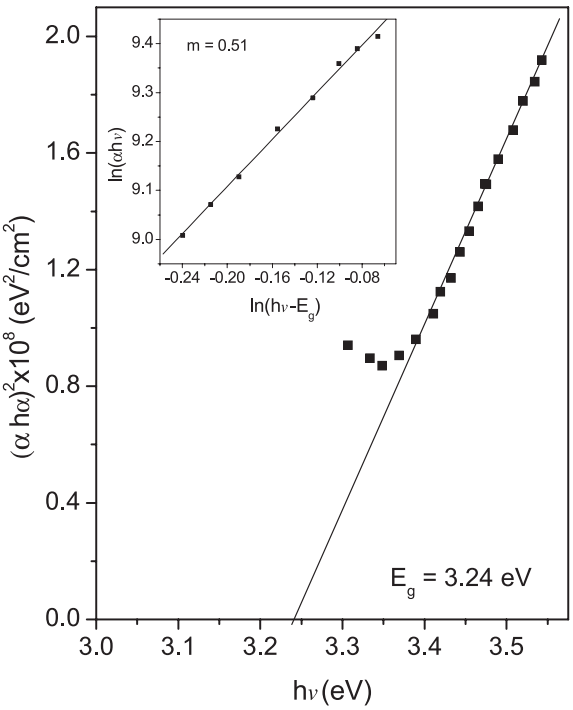

Fig. 1. Plot of $(\alpha h\nu)^2$ versus $h\nu$ for a representative film (undoped GaN).

Table 1. Values of band gap (E_g), barrier height (E_b) at the grain boundaries, strain ($\delta a/a$) and stress (S) in undoped, Be-doped and Si-doped GaN films deposited at different substrate temperature during deposition.

Thin film description	$T_s(K)$	E_g(eV)	E_b(eV)	$\delta a/a$ ($\times 10^4$)	S(GPa)	Hardness (GPa) $x = 10\%$
Poly GaN	623	3.22	1.77	19.69	0.549	4.72
	523	3.26	1.68	13.98	0.390	4.48
	423	3.37	1.66	8.28	0.231	4.15
	300	3.40	1.62	5.27	0.147	3.91
Be GaN	623	3.067	1.72	18.91	0.528	4.69
	523	3.179	1.67	13.45	0.375	4.45
	423	3.235	1.59	7.99	0.223	4.13
	300	3.28	1.55	4.00	0.112	3.78
Si GaN	623	3.18	1.7	10.27	0.287	4.28
	523	3.27	1.3	9.83	0.274	4.25
	423	3.35	0.7	8.95	0.249	4.19
	300	3.42	0.3	7.97	0.223	4.13

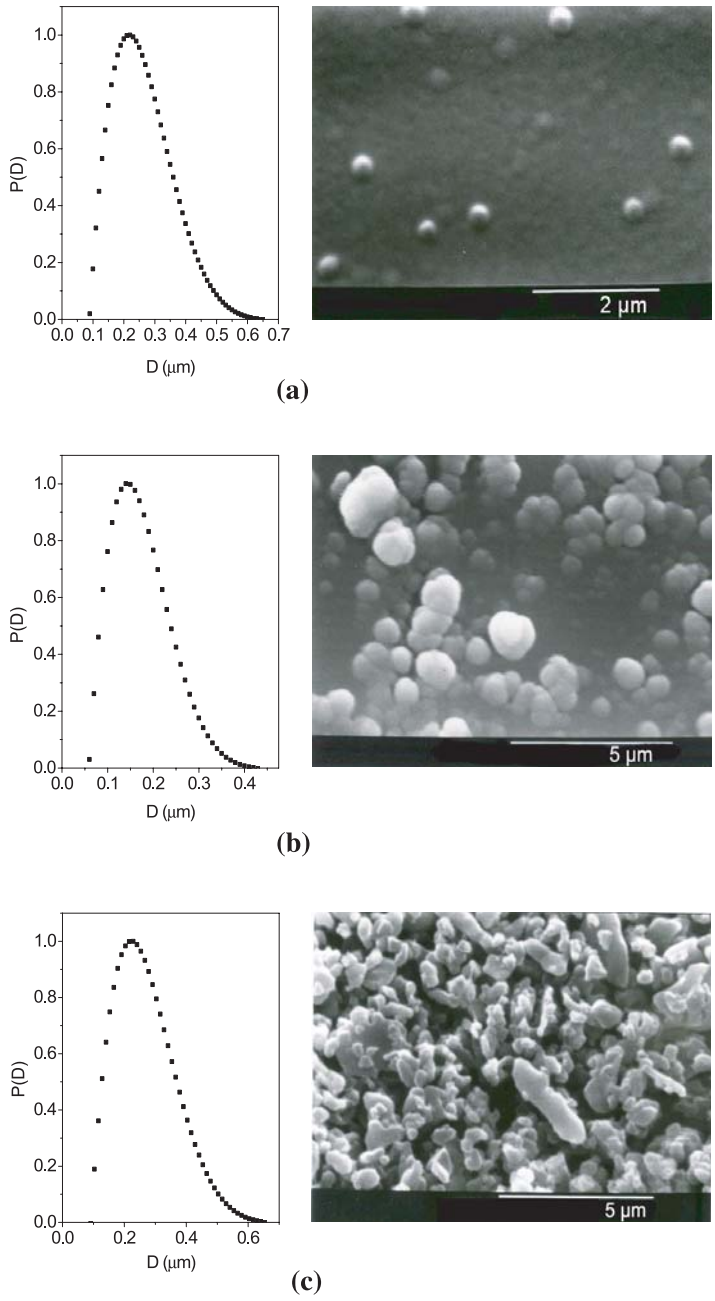

Fig. 2. SEM micrographs of GaN films deposited at 623 K: (a) undoped; (b) Be-doped and (c) Si-doped.

the doped films determined from optical measurement were found to be lower than the band gaps of bulk gallium nitride. This is basically due to the band bending arising out of the presence of grain boundary states and acceptor/donor levels due to doping. Presence of mixed phases present in the films deposited at intermediate temperatures was confirmed by XRD traces (not shown here).

3.2 Microstructural properties

Surface morphology and grain distribution in these films were studied by scanning electron microscopy. Figure 2 shows the micrographs of three representative films deposited at ∼623 K. It may be observed that undoped films had a smoother and compact surface while the Be-doped ones had nearly spherical grains. Contrary to both, the Si-doped films had oblong grains. The grain sizes obtained from the SEM pictures (Figs. 2a, 2b, 2c) are 0.36 μm, 0.37 μm 0.5 μm respectively. The grain sizes (D) of the three representative films undoped, Be-doped and Si-doped GaN obtained from optical measurements were found to be 0.36 μm, 0.24 μm and 0.37 μm respectively which tallied well with that obtained from SEM studies.

3.3 Determination of stress

We have considered the optical absorption in the films just below the band gap (E_g) since the grain boundary phenomena in polycrystalline films are known to influence the optical absorption band tails. Generally, for large grain

polycrystalline material there is a sharp change of the absorption coefficient at the band edge (E_g) similar to that observed in a crystalline material while for films with moderate grains, the absorption coefficient vs. energy plot is not so sharp. In fact, the variation of the optical absorption coefficient (α) with energy ($h\nu$) below the band edge of a polycrystalline material will contain the information of the grain boundary parameters like density of defect states (Q_t), average built-in-electric field (F_{av}), etc.

In general, polycrystalline films are known to be the aggregates of randomly distributed grains and grain boundary regions. The latter contain a large amount of defect states which become charged after trapping free carriers from the neighbouring grains. Besides this random distribution of the intrinsic defect states at the grain boundary regions of the film, there will be considerable amount of thermal stress due to the mismatch of thermal expansion coefficients of the film (α_{film}) and substrate (α_{subs}). As a result, the potential and hence the band gap (E_g) would have a fluctuating nature which may culminate in the existence of additional indirect optical transitions below the fundamental band gap of the material. As the details of the processes have already been reported elsewhere [13,23,24], a brief outline is presented here. Let us assume the presence of Q_t amount of defect states at the grain boundary regions of a polycrystalline film. This will result in a fluctuating potential with average height E_b and internal electric field F_{av} as given by [25]:

$$eF_{av}\lambda_D = E_b \tag{4}$$

where

$$F_{av} = eQ_t/\varepsilon \tag{5}$$

e is the electronic charge, ε is the average dielectric constant and λ_D is the Debye screening length [16] which is inversely proportional to $\sqrt{N_D}$, where N_D is the free carrier concentration. Moreover, we have considered a Gaussian type of fluctuating band gap [13,23]:

$$D(E_g) \sim \exp\left[-\left(E_g - \bar{E}_g\right)^2 / 2\sigma_1^2\right] \tag{6}$$

which may be associated with a correlation function $B(r)$

$$B(r) = {\sigma_1}^2 \exp\left(-r^2 / {L_c}^2\right). \tag{7}$$

Here, $\bar{E}_g$ is the average value of the fluctuating band gap, L_c is the correlation length and σ_1 is a disorder at the grain boundary region. This disorder parameter σ_1 which physically indicates the rms value of the fluctuating antiparallel displacement of the valance and the conduction band edges from those of the ideal crystalline lattice, may be related to the residual total strain ($\delta a/a$) by the expression [13,23]:

$$\sigma_1^2 = (\bar{E}_g)^2 4(\delta a/a) \tag{8}$$

where the total strain ($\delta a/a$) is the sum of the intrinsic strain $(\delta a/a)_{in}$, and the thermal strain $(\delta a/a)_{th}$ and may be expressed as:

$$\left(\frac{\delta a}{a}\right) = k(T^* + T)/4Mv^2 \tag{9}$$

$$\text{where} \quad \left(\frac{\delta a}{a}\right)_{th} = \alpha_{film} - \alpha_{subs}(T_s - T). \tag{10}$$

The parameters M, v, T_s, and T correspond to the atomic (or molecular) mass, velocity of sound in the material, the deposition temperature and the temperature of optical measurement ($T \sim 300$ K), respectively. T^* used here is the temperature equivalent of the intrinsic disorder due to defect states present at the grain boundary region. The strain component $(\delta a/a)_{in}$ represents the contribution due to the combined effects of intrinsic defect states and phonons (originated from the thermal lattice vibration both in the grain and grain boundary regions), while the other strain parameter $(\delta a/a)_{th}$ corresponds to the difference of thermal expansion coefficients of the film and the substrate.

For a fluctuating band gap as given by equation (6) the general expression for the absorption coefficient due to indirect transitions between different sites (with the conservation of carrier's energy only) is [13]:

$$\alpha\,(h\nu) \sim \exp\left[(h\nu - E_0)/E\right] \phi\,(h\nu)\,. \tag{11}$$

The different parameters used here are $E_0 = E_g - \sigma_1^2/2E$ with $E = h\sigma_1^2 \Big/ \left(6m^* L_c^2\right)^{1/3}$ and $\phi(h\nu)$ is a slow varying function given by:

$$\phi(h\nu) = E_g^{-1} \int_{h\nu}^{\infty} dE_g \exp\left(-\sigma_1^2/2E'\right). \tag{12}$$

The explicit form of the parameter E' which represent the Urbach edge is given by [13,25]:

$$E' = \{\hbar^2\sigma^2/[6L_c^2(m*/m_0)]\}^{1/3} \tag{13}$$

where m^*/m_0 is the effective mass ratio (m_0 being the free electron mass). In the photon energy range $h\nu < E_g$ which is of special interest to us here, $\phi(h\nu)$ is almost constant.

The films were deposited at four different substrate temperatures (300, 423, 523 and 623 K). The below band gap experimental plots of normalized absorption coefficients (α/α_o) for the three representative films of undoped, Be-doped and Si-doped GaN deposited at $T_s \sim 623$ K are shown in Figures 3a–c respectively. As the contribution to absorption due to the thermal disorder for any material at a specific temperature (say the room temperature at which optical absorption has been recorded) is fixed, the ultimate shape of (α/α_o) vs. ($E_g - h\nu$) plot will depend on the amount of the intrinsic disorder or the density of the defect states present in the film. Using equation (11) different grain boundary parameters (σ_1, Q_t and F_{av}) were estimated from the best fit theoretical curve (shown in Figure 3 by solid lines) corresponding to the experimental data of (α/α_0) vs. ($E_g - h\nu$), α_o being

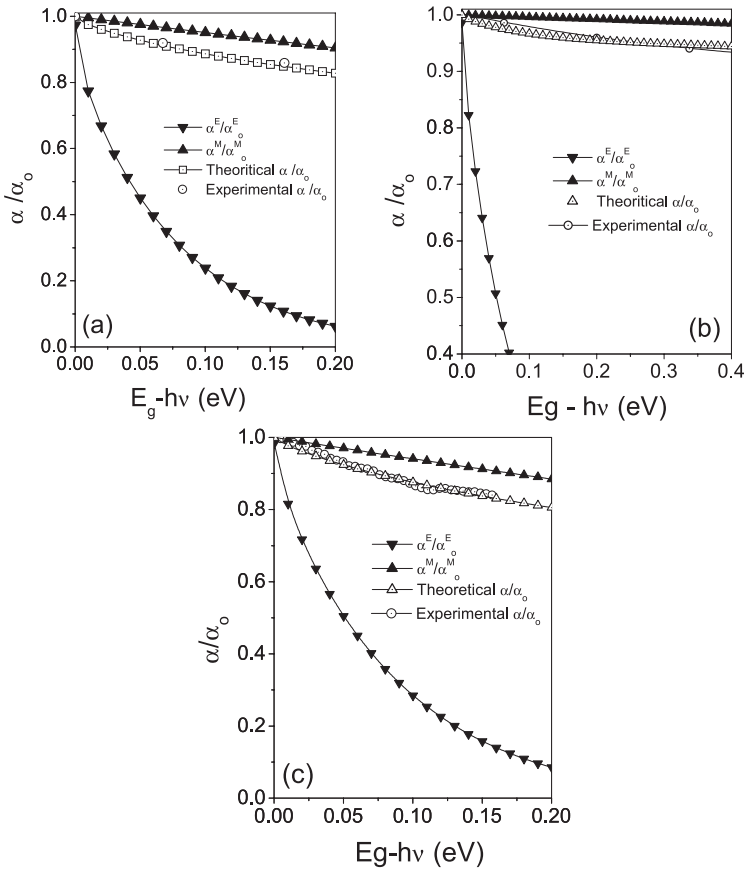

Fig. 3. Variation of α/α_o versus $(E_g - h\nu)$ for representative films of: (a) undoped GaN, (b) Si-doped GaN and (c) Be-doped GaN deposited at 623 K.

Table 2. Values of different parameters used for the theoretical simulation.

Film reference	v ($\times 10^{-3}$ ms^{-1})	Y ($\times 10^{9}$ Nm^{-2})	σ	a (Å)	$m*/m_0$
GaN	6.9	181	0.352	4.52	0.13

the value of α at E_g. The different parameters used for the above theoretical simulation are given in Table 2. It may be mentioned here that σ_1 and $(\delta a/a)_{in}$ are the two most sensitive parameters in this non-destructive curve fitting technique. The corresponding variations of the strain $(\delta a/a)$ for three sets of polycrystalline GaN films with substrate temperature (T_s) during deposition are shown in Figure 4.

From the experimentally obtained values of residual strain $(\delta a/a)$, and by knowing the standard values of Youngs modulus Y (Nmm^{-2}) and the Poissons ratio σ_p for a given film material, the true stress (S) can be obtained using the standard equation for elasticity:

$$S = [Y/(1 - \sigma_P)](\delta a/a) \qquad (14)$$

Stresses in the films thus evaluated are shown in Figure 5. It may be noted that the stress increased sharply for films deposited at higher temperature for undoped and Be-doped GaN films while Si-doped GaN films did not indicate such a change. The stress varied between 0.2 to 0.3 GPa for Si-doped films.

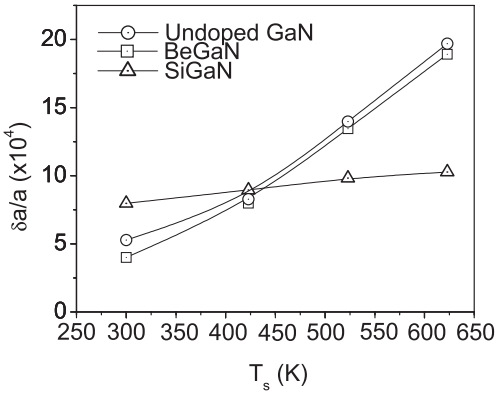

Fig. 4. Variation of $\delta a/a$ for different films deposited at different substrate temperature during deposition.

Now, in the presence of Peierls potential, the lattice distortion cannot move easily under a small externally applied stress field. A critically applied stress (S^*) has to be applied just to move the dislocation over this potential without any assistance from thermal or quantum lattice vibration. This ultimate tensile stress also called the "Peierls Stress" can be obtained from the discrete

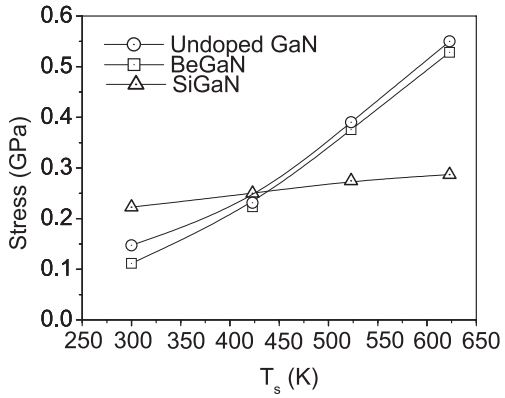

Fig. 5. Variation of stress for different films deposited at different substrate temperature during deposition.

dislocation model [26] and is given by:

$$S^* = \{2\mu/(1-\sigma_P)\}\exp\{-\pi h/[(1-\sigma_P)b]\} \quad (15)$$

where $\mu = Y/[2(1+\sigma_p)]$ is the shear modulus, $b \approx a[1+\delta a/a]$, the tensile stress, which represents the magnitude of the Burger vector, denoting the slip direction and h is a quantity, of the order of the lattice parameter which represents the spacing across the slip plane.

It is known that a relation between the ultimate tensile stress (S^*) and the Vickers hardness (H_ν) corresponding to an arbitrary indentation strain (x %) could be expressed as [27–29]:

$$H_V = 2.9S^*/(36.8n_c/x)^{n_c} \quad (16)$$

where n_c, the strain hardening coefficient, can be obtained by solving the equation

$$(S/S^*) = [2.718(\delta a/a)/n_c]^{n_c}. \quad (17)$$

A simple computer simulation was carried out to obtain the Vickers hardness of undoped, Be doped and Si doped polycrystalline GaN thin film. From equations (14 and 15), one obtains:

$$S/S^* = \{(\delta a/a)(1+\sigma_P)\}\exp\{(\pi/(1+\delta a/a))(1-\sigma_P). \quad (18)$$

Knowing the values of Youngs modulus Y, Poissons ratio σ_p, and using equation (17), equation (18) was solved using the Newton Raphson iterations technique to obtain the strain hardening coefficient (n_c) correct upto the desired decimal places and this n_c was subsequently utilized in equation (16) along with calculated S^* to get the Vickers hardness for the concerned materials. The variation of theoretically obtained Vicker's hardness for the films deposited at different temperature are shown in Figure 6 and tabulated in Table 1. It may be seen that the undoped GaN films had the highest hardness compared to the doped ones. Si-doped GaN films had the lowest hardness.

It will be interesting to compare the above observation with the measurements of hardness with a fully automated FISCHERSCOPE depth sensing indentometer.

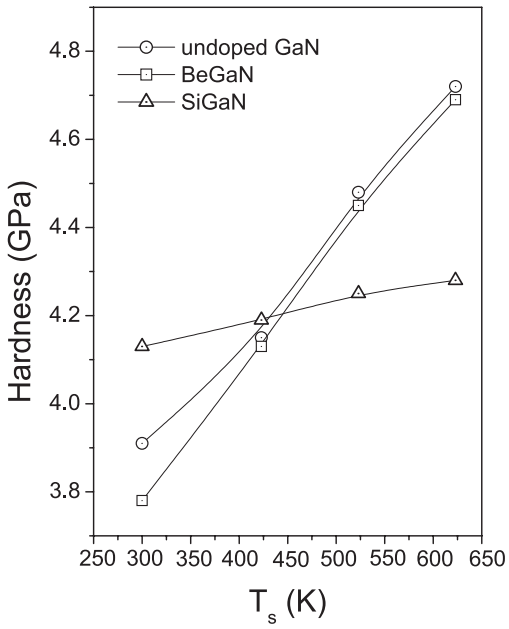

Fig. 6. Calculated hardness values of the undoped and doped GaN films from optical measurement.

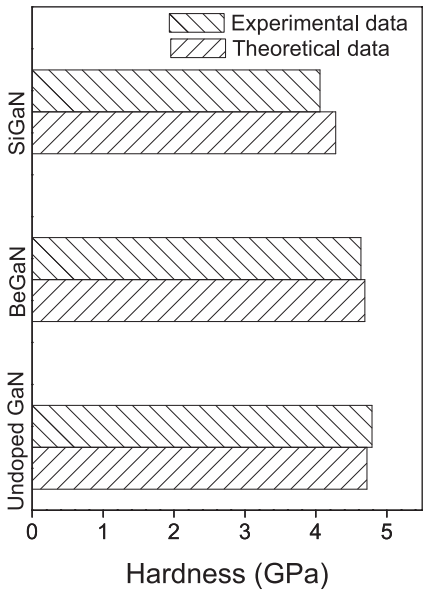

Fig. 7. Comparison of the hardness as determined from optical studies and direct measurement for representative doped and undoped GaN films.

The hardness of the GaN films was determined from the measured indentation curve assuming a perfect geometry of the diamond Vickers indenter and making the correction for the tip blunting) by extrapolating the unloading curve from the maximum applied load P_{max} to zero load (not shown here). The hardness evaluated as above for a load ∼3 mN are shown in Figure 7 for three representative GaN films (undoped, Be-doped and Si-doped) deposited at $T_s = 623$ K along with that evaluated from optical measurement. It may be observed that undoped GaN has the highest hardness (∼5000 N/mm^2) followed by Be-doped

with a hardness of 4635 N/mm^2. Si-doped films had lower hardness ∼4059 N/mm^2. This result is in conformity with that obtained from the optical measurement.

4 Conclusion

Polycrystalline GaN films (doped and undoped) were deposited by R.F. sputtering onto fused silica substrates at various deposition temperatures ranging from 300 K to 623 K. Residual stresses in these films were evaluated from the band tail of the absorption spectra as well as from direct measurements of hardness by commercially available depth sensing indentometer. It was observed that undoped GaN films had the highest hardness followed by that for Be-doped and Si-doped films.

Three of us MPC, RKR and SRB wish to thank the Council of Scientific and Industrial Research, Government of India, for granting them fellowship for executing this programme. The authors are indebted to Dr. A. Mukherjee, Central Glass & Ceramic Research Institute, Calcutta 700032, India for his assistance in recording the hardness of the films.

References

1. J.P. Park, Maria, J.J. Cuomo, Y.C. Chang, J.F. Muth, R.M. Kolbas, R.J. Nemanich, E. Carlson, J. Bumgarner, Appl. Phys. Lett. **81**, 1797 (2002)
2. S. Yagi, S. Suzaki, T. Iwanaga, Jpn. J. Appl. Phys. **40**, L349 (2002)
3. V.A. Christie, S.I. Liem, R.J. Reeves, V.J. Kennedy, A. Markwitz, S.M. Durbin, Current Appl. Phys. **4**, 225 (2004)
4. P. Seong-Eun, L. Sung-Mook, O. Byungsung, J. Cryst. Growth **250**, 349 (2003)
5. H. Tampo, H. Asahi, Y. Imanishi, M. Hiroki, K. Ohnishi, K. Yamada, K. Asami, S. Gonda, J. Cryst. Growth **227**, 442 (2001)
6. M. Hiroki, H. Asahi, H. Tampo, K. Asami, S. Gonda, J. Cryst. Growth **209**, 387 (2000)
7. C. Kisielowski, J. Kruger, S. Ruvimov, T. Suski, J.W. Ager III, E. Jones, Z. Lilental-Weber, H. Fujii, M. Rubin, E.R. Weber, M.D. Bremser, R.F. Davis, Phys. Rev. B **54**, 17745 (1996)
8. O. Lagerstedt, B. Monemar, Phys. Rev. B **19**, 3064 (1979)
9. Y. Kim, R. Klockenbrink, C. Kisilowaski, I. Krueger, D. Corlatan, Sudhir G.S., Y. Peyrot, Y. Cho, M. Rubin, E.R. Weber, Mat. Res. Soc. Symp. Proc. **482**, 217 (1998)
10. G.H. Leusnik, T.G.M. Oosterlaken, G.C.A.M. Janssen, S. Radelaar, J. Appl. Phys. **74**, 3899 (1993)
11. G. Bentoumi, A. Deneuville, E. Bustarret, B. Daudin, G. Feuillet, Thin Solid Films **364**, 114 (2000)
12. B.K. Ghosh, T. Tanikawa, A. Hashimoto, A. Yamamoto, Y. Ito, J. Cryst. Growth **249**, 422 (2003)
13. A.B. Maity, S. Chaudhuri, A.K. Pal, Phys. Stat. Solidi, (b) **183**, 185 (1994)
14. P. Dow, D. Redfield, Phys. Rev. B **1**, 3358 (1970)
15. M. Bujatti, F. Marcelja, Thin Solid Films **11**, 249 (1972)
16. A.B. Maity, M. Basu, S. Chaudhuri, A.K. Pal, J. Phys. D. **28**, 2547 (1995)
17. M.F. Doerner, W.D. Nix, J. Mater. Res. **1**, 601 (1986)
18. S. Veprek, S. Mukherjee, P. Karvankova, H.D. Männling, J.L. He, K. Moto, J. Prochazka, A.S. Argon, Thin Solid Films **436**, 220 (2003)
19. W.C. Oliver, G.M. Pharr, J. Mater. Res. **7**, 1564 (1992)
20. D. Bhattacharyya, S. Chaudhuri, A.K. Pal, Vacuum **43**, 313 (1992)
21. J.C. Manifaciar, M. de Muricia, J.P. Fillard, E. Vicario, Thin Solid Films **41**, 127 (1977)
22. D. Bhattacharyya, S. Chaudhuri, A.K. Pal, Vacuum **44**, 797 (1993)
23. J. Szczyrbowski, Phys. Stat. Solidi b **105**, 515 (1981)
24. V.I. Gavrilenko, Phys. Stat. Solidi b **139**, 457 (1987)
25. A.B. Maiti, D. Bhattacharyya, S. Chaudhury, A.K. Pal, Vacuum **46**, 319 (1995)
26. K. Oshawa, H. Koizumi, H.O.K. Kirchnen, T. Suzuki, Phil. Mag. A **69**, 171 (1994)
27. D. Tabor, J. Inst. Met. **79**, 1 (1951)
28. S.C. Chang, M.T. Jahn, C.M. Wan, J.Y.M. Lee, T.K. Hsu, J. Mater. Sci. **11**, 623 (1976)
29. M.O. Lai, K.B. Lim, J. Mater. Sci. **26**, 2031 (1991)